Available online at www.sciencedirect.com
SCIENCE DIRECT
Polymer 46 (2005) 8321–8330
polymer
www.elsevier.com/locate/polymer

Cocrystallization mechanism of poly(3-alkyl thiophenes) with different alkyl chain length

Susmita Pal, Arun K. Nandi*

Polymer Science Unit, Indian Association for the Cultivation of Science, Jadavpur, Kolkata 700032, India

Received 18 February 2005; received in revised form 10 June 2005; accepted 14 June 2005
Available online 19 July 2005

Abstract

The crystallization rates of poly(3-alkyl thiophene) (P3AT) cocrystals having different alkyl chain length (e.g. hexyl and octyl) of the components are measured using differential scanning calorimetry (DSC) technique. Two pairs of cocrystals with varying compositions of the components viz. poly(3-octyl thiophene) (P3OT(R), regioregularity 89 mol%) and poly(3-hexyl thiophene) [P3HT(R), regioregularity 92 mol% and P3HT-2 regioregularity 82 mol%] are used. In both the systems the isothermal temperature range (TR) in the same time scale of crystallization is found to decrease with increasing alkyl chain length in the blends. The crystallization rate at the same T_c decreases with increasing alkyl chain length P3AT concentration and the Avrami exponent values of cocrystals are same with those of the component values. The low Avrami exponent values (0.23–1.16) in all the samples suggest the presence of rigid amorphous portion which can not diffuse out quickly from the crystal growth front (soft impingement). Analysis of crystallization rate using Laurintzen–Hoffman (L–H) growth rate theory indicates that there is regime-I to regime-II transition in all the samples. The product of lateral (σ) and end surface energy (σ_e) values are found to decrease with increasing the concentration of longer alkyl chain P3AT in the blend. Analysis of σ values according to a theory of Hoffman et al. [Hoffman JD, Miller RL, Marand H, Rotiman DR. Macromolecules 1992;25:2221. [14]] indicates that there is chain extension of the components in the melt of the blends, however, the entropy of cocrystallization has different sign to the two systems. Cocrystallization in P3HT(R)/P3OT(R) system is an entropy driven process but that in P3HT(2)/P3OT(R) system is entropy forbidden process. A possible explanation of cocrystallization in the later system has been attributed from small interaction between the components.

Keywords: Poly(3-hexyl thiophene); Poly(3-octyl thiophene); Crystallization kinetics

1. Introduction

Poly(3-alkyl thiophenes) (P3ATs) are important members of conducting polymer family and are highly used in electronic and opto-electronic applications [1]. The polymers are not completely isoregic and the pendent alkyl chain length may also vary. Both the size of the pendent alkyl group and regioregularity of the main chain have strong influence on the physical and conductivity properties of this important polymer [1–6]. We have studied the cocrystallization of the P3ATs with an aim to produce tailor made materials of desired properties without going to much laborious synthesis [7]. We have shown that the p3AT sample of same regioregularity can cocrystallize for an alkyl chain length difference of two carbon atoms and the cocrystallization between poly(3-hexyl thiophene) (P3HT) and poly(3-octyl thiophene) (P3OT) can be extended to a regioregulatity difference of 7 mol%. In this article we want to delineate the cocrystallization mechanism of the above P3ATs from the crystallization rate measurement using differential scanning calorimetery (DSC) technique (Scheme 1).

There are some reports on the crystallization kinetics of the cocrystals in the literature. Ree observed an intermediate crystallization rate in the cocrystals of linear low-density polyethylene and ultra high molecular weight polyethylene at the same isothermal crystallization temperature (T_c) [8]. But Irragori et al. observed an enhanced growth rate of cocrystals between linear and branched polyethylene at same T_c [9]. Tashiro et al. measured the crystallization rate of polyethylene blends and observed higher crystallization

* Corresponding author. Tel.: +91 33 247 34971; fax: +91 33 247 32805.
E-mail address: psuakn@mahendra.iacs.res.in (A.K. Nandi).

0032-3861/$ - see front matter © 2005 Elsevier Ltd. All rights reserved.
doi:10.1016/j.polymer.2005.06.048

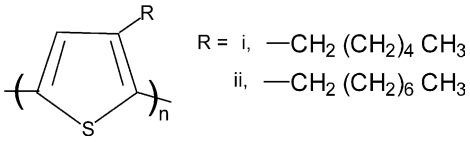

Scheme 1. Structure of poly(3-alkyl thiophene).

rate of cocrystals at the same undercooling using time resolved FTIR and time resolved SAXS instruments [10,11]. Similar increase in growth rate and crystallization rate was observed for cocrystals of different head to head (H–H) defect content poly(vinylidene fluoride) (PVF_2) samples and also for cocrystals of vinylidene fluoride–tetrafluoroethylene copolymers at same undercooling [12,13]. The kinetic data of the cocrystallization process was analyzed using a recent theory of Hoffman et al. [14] and chain extension in the melt of the blend causing easier crystallization of cocrystals at same undercooling was concluded in both systems. The thermodynamic analysis of the kinetic data also concluded that in both systems cocrystallization is an entropy-driven process [12,13].

Here we shall attempt to understand the mechanism of cocrystallization of P3ATs of varying alkyl chain length of the pendent alkyl group from the crystallization kinetics study. The crystallization rate, isothermal temperature range (T_R) for same time scale of crystallization, Avrami exponents (n), etc. will be compared between the cocrystals with varying composition of their components. It is now established from X-ray and scanning tunnelling microscopy studies that P3ATs crystallize in chain folded fashion [15,16]. So the kinetic data will be analyzed using Lauritzen–Hoffman (L–H) growth rate theory of chain folded polymer crystals [17]. From the lateral and end surface energies of the cocrystals, evaluated from the above analysis, attempt will be made to understand the thermodynamics of the blend both at the melt and at the solid state.

2. Experimental

2.1. Samples

Two types of P3HT samples, e.g. regioregular (P3HT(R)) and regioirregular (P3HT-2) samples and regioregular P3OT (P3OT(R)) sample were used in the work. The regioregular samples were purchased from Aldrich Chemical Co. USA and regioirregular poly(3-hexyl thiophene) (P3HT-2) sample was synthesized from the chloroform solution in the laboratory as earlier [7]. The characteristics of the samples used in the work are presented in Table 1 [7]. Blends were prepared by homogeneously mixing appropriate amount of the components in chloroform solution and then drying off the solvent. The films were finally dried in vacuum at 60° for 3 days.

Table 1
Characteristics of the samples

P3AT samples	Source	$\bar{M}_w \times 10^{-4}$	H–T regioregularity	Equilibrium melting point (°C) (T_m^0)[a]
P3HT(R)	Aldrich	8.7	92	300
P3OT(R)	Chem. Co. USA	14.2	89	270
P3HT-2	Prepared	10.6	82	290

[a] From Ref. [28].

2.2. Cocrystallization kinetics study

A Perkin–Elmer differential scanning calorimeter (DSC-7) fitted with intracooler-1 and working under nitrogen atmosphere was used in the work. The instrument was calibrated with indium before each set of experiment. To understand the cocrystallization in these systems ~5 mg of the blend samples were encapsulated in aluminum pans and were melted in nitrogen atmosphere at 250 and 220 °C for 5 min for P3HT(R) and P3HT-2 blends, respectively. They were then quenched to −30 °C and heated at the rate of 20°/min to the temperatures stated above. For the dynamic cooling experiments they were cooled from the melt at the same melting temperatures at the rate of 5°/min.

The crystallization kinetics of the P3ATs and their cocrystals were studied using about 5 mg of the samples in aluminium pans and melting them at 250 and 220 °C for five min for P3HT(R) and P3HT-2 blends, respectively. They were quenched at the rate of 200 °C/min to the predetermined isothermal crystallization temperature (T_c) where they were crystallized for different times. The samples were then heated from the T_c at the heating rate of 10°/min without cooling. The enthalpy of fusion (ΔH) and the melting points were measured by a computer attached to the instrument using PC-series DSC-7 multitasking software (version 3.2). The percentage crystallinity was calculated from the ratio of ΔH and ΔH_u^0 (enthalpy of fusion of perfect crystal) taking $\Delta H_u^0 = 99$ J/g for P3HT, 74 J/g for P3OT [18] and arithmetic average of the component values for the blends.

3. Results and discussion

The formation of cocrystals in these systems is clarified from Fig. 1(a) and (b) where representative thermograms of heating and cooling processes of P3OT(R)/P3HT(R) and P3OT(R)/P3HT(2) systems are shown. In the former system the melting peak at 208 °C is for the main chain crystals and the single peak corresponds to cocrystallization of the components at this blend composition as they have a difference of apparent melting point of 58 °C [7]. In the P3OT(R)/P3HT(2) system the single melting peak definitely corroborates cocrystallization as the components have an

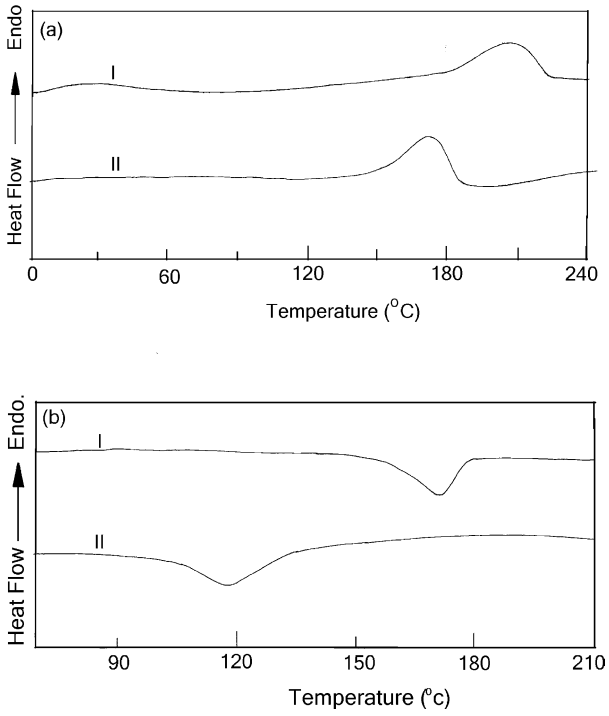

Fig. 1. (a) Melting endotherm of the melt-quenched samples of (I) P3OT(R) /P3HT(R) blend ($W_{P3OT(R)}=0.40$) and (II) P3OT(R)/P3HT-2 blend ($W_{P3OT(R)}=0.50$) at the heating rate of 20°/min. (b) Crystallization exotherms of the above samples (I and II) at the cooling rate of 5°/min from the respective melt at 250 and 220 °C, respectively.

apparent melting point difference of 18 °C [7]. The cooling thermograms of both the systems (Fig. 1(b)) exhibit single crystallization peak supporting cocrystallization in the samples and it is also further confirmed from the wide angle X-ray study reported earlier [7]. However, it may be noted that in the heating thermogram at lower temperature (~30 °C) there is a broad hump for the P3OT(R)/P3HT(R) system probably arising from the melting of the side chain crystals [18]. But this is absent in the other system probably for the absence of side chain crystallization due to large regioregularity difference (7 mol%) between the components.

3.1. Crystallization isotherms

The crystallization kinetics of the P3AT cocrystals are studied from the isothermal crystallization in DSC for predetermined times and melting these crystals from that isothermal temperature. Representative melting endotherms of P3OT(R)/P3HT(R) blend ($W_{P3OT(R)}=0.50$) crystallized at 214 °C are shown in Fig. 2 for different times of crystallization. The enthalpy of fusion of these crystals are measured and plotted with time to get the crystallization isotherms. In Fig. 3(a)–(c) the crystallization isotherms of cocrystals of P3OT(R)/P3HT(R) systems are presented. Like the crystallization isotherms of other polymers here also a sigmoidal rise of crystallization isotherms is observed

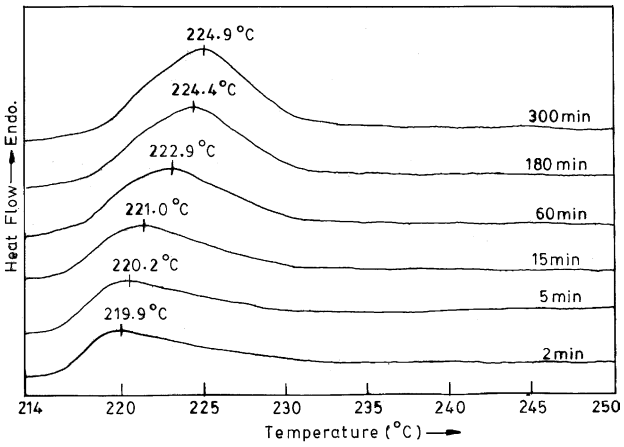

Fig. 2. Representative DSC thermograms of P3OT(R)/P3HT(R) blend ($W_{P3OT(R)}=0.50$) crystallized at 214 °C for indicated crystallization times.

at each temperature indicating autocatalytic nature of the crystallization process. The isothermal crystallization temperatures of P3OT(R) are much lower than that of P3HT(R). This indicates that crystallization of P3AT is difficult with increasing alkyl chain length. In Fig. 4(a)–(d) the crystallization isotherms of P3OT(R)/P3HT-2 system are presented. Here the isothermal temperature range for the same time scale of crystallization is almost same in the blends. The isothermal temperature range for the same time scale of crystallization is plotted with weight fraction of P3OT(R) in both the systems and is shown in Fig. 5. In P3HT(R)/P3OT(R) system the line is not completed as there was no cocrystal formation at the composition $W_{P3OT(R)}=0.86$ [7]. A sharp decrease of isothermal temperature range with increasing P3OT(R) is observed in the P3HT(R)/P3OT(R) system whereas a gradual decrease of the same is observed in P3OT(R)/P3HT-2 systems. P3HT(R) is more easily crystallizable than P3HT-2 sample, which in turn is more easily crystallizable than that of P3OT(R). The reason for the former may be attributed to higher regioregularity while that for the later is due to both regioregularity and alkyl chain length difference. The large difference of isothermal temperature region between P3HT(R) and P3OT(R) is due to the alkyl chain length difference i.e. longer the alkyl chain length greater is the hindrance to crystallization. A better comparison can be obtained from Fig. 6 where crystallization rate [$1/\tau_{.01}$, $\tau_{.01}$ is the time of crystallization to obtain 1% crystallinity] is plotted with P3OT(R) content. It is apparent from the figure that crystallization rate decreases with increasing P3OT(R) content for each isothermal temperature. In the P3HT(R)/P3OT(R) system the regioregularity of the samples are same so the effect is mainly due to the chain length difference of the alkyl group and it clearly indicates a significant decrease of crystallization rate with increasing P3OT(R) in the blend. In the other system P3HT-2 is of lesser regioregularity than that of P3OT(R) so there is a combined effect of

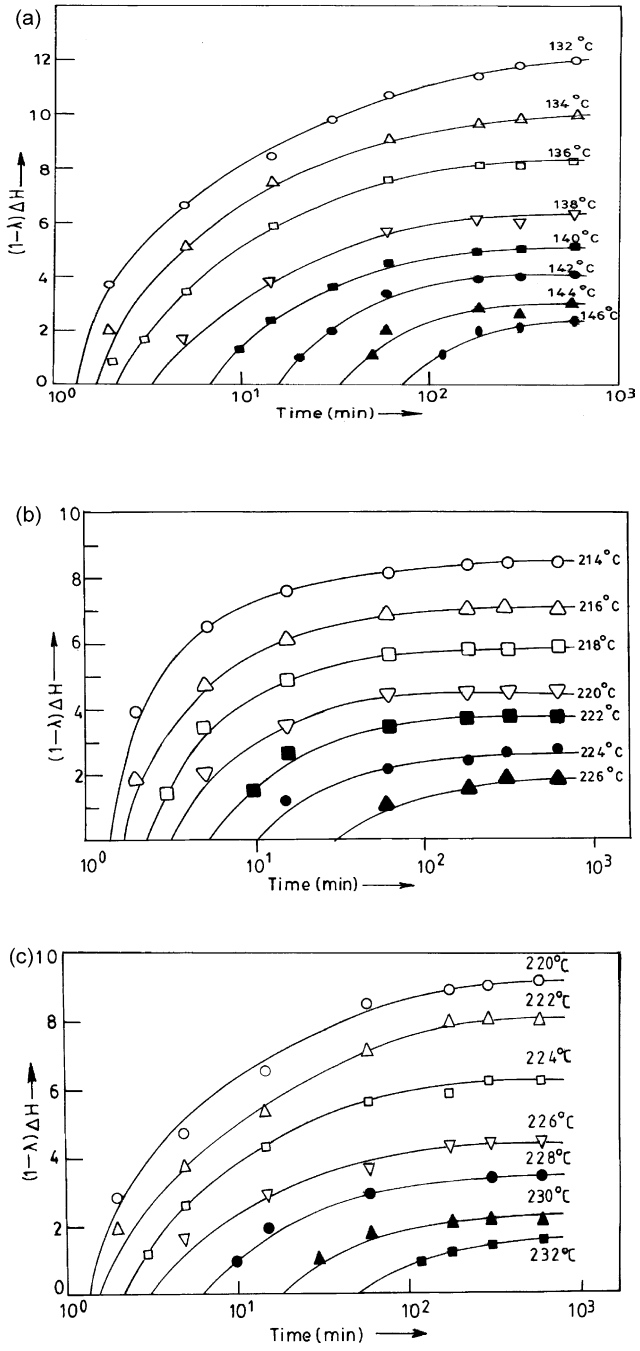

Fig. 3. Crystallization isotherms at indicated temperatures of P3OT(R) /P3HT(R) systems: (a) $W_{P3OT(R)}=1.0$ (b) $W_{P3OT(R)}=0.5$, (c) $W_{P3OT(R)}=0.0$.

regioirregularity and alkyl chain length and a sharper decrease of crystallization rate is observed.

3.2. Avrami analysis

To elucidate the overall crystallization mechanism the Avrami equation (Eq. (1)) is applied [19–21]:

$$1-\lambda(t)=1-\exp(-kt^n) \tag{1}$$

where $1-\lambda(t)$ is the crystallinity at time t, k is the overall rate constant and n is the Avrami exponent which denotes the nature of nucleation and growth process. The slope of the double logarithmic plot of $1-\lambda(t)$ with t at low levels of crystallinity yields the value of n [21]. The n values of cocrystals are presented in Table 2 and it varies from 0.23 to 1.16. The n values are almost same with those of the component values indicating that the crystallization mechanism of the cocrystals are similar to that of the components. Nascimento et al. reported similar n values of poly(3-methyl thiophene) from an electron spin resonance study [22]. Such n values are usually found in condis crystals and liquid crystalline polymers [23,24] and recently in the crystallization of vinylidene fluoride–tetrafluoro ethylene copolymers similar low n values are also reported [25].

Usually for polymer crystallization n has value of 2 or 3 indicating two or three dimensional nucleation of the crystal nucleus. However, fractional values of n also exist due to secondary crystallization or crystal perfection [24]. To explain the lower n values (<1) Cheng and Wunderlich [23] modified the Avrami equation by considering the applicability of the two assumptions of negligible nuclei volume fraction and linear crystal growth rate used in deriving Eq. (1). In some rigid chain polymers and condis crystals a non-negligible volume fraction of nuclei does exist contributing an important role in the crystallization mechanism. Also in rigid chain polymers a major fraction remains as amorphous phase and cannot diffuse out quickly from the crystal growth front causing a decrease in crystal growth rate (soft impingement). Considering these factors the Avrami expression has been modified as [23]:

$$1-\lambda(t)=1-\exp[-kt^{[n(m+1)+p]}] \tag{2}$$

where m and p are negative quantity. The negative value of m signifies that crystal growth rate (G) decreases with increase in time (t) ($G=G_0t^m$) for soft impingement and negative value of p signifies that number of active nuclei (N) decreases with increase in time ($N(t)=N_0t^p$) due to the already presence of large volume fraction of nuclei, some of them become exhausted with time. As both m and p are negative the Avrami exponent value becomes much lesser than the conventional values of 2 or 3.

In the present system, soft impingement is occurring as there is large amount of amorphous portion ($\sim$90%, cf. Figs. 3 and 4) in the material arising from the rigidity of the P3AT chain. Also significant nucleation occurs through the spontaneous interdigitation of the side chains [18] and these nuclei cannot grow much due to rigidity of the chain yielding very low crystallinity. So from the above analysis it may be concluded that the low value of n in this system is arising from both the non-negligible volume fraction of the nuclei and also from the soft impingement of the growing crystal with the rigid amorphous portion.

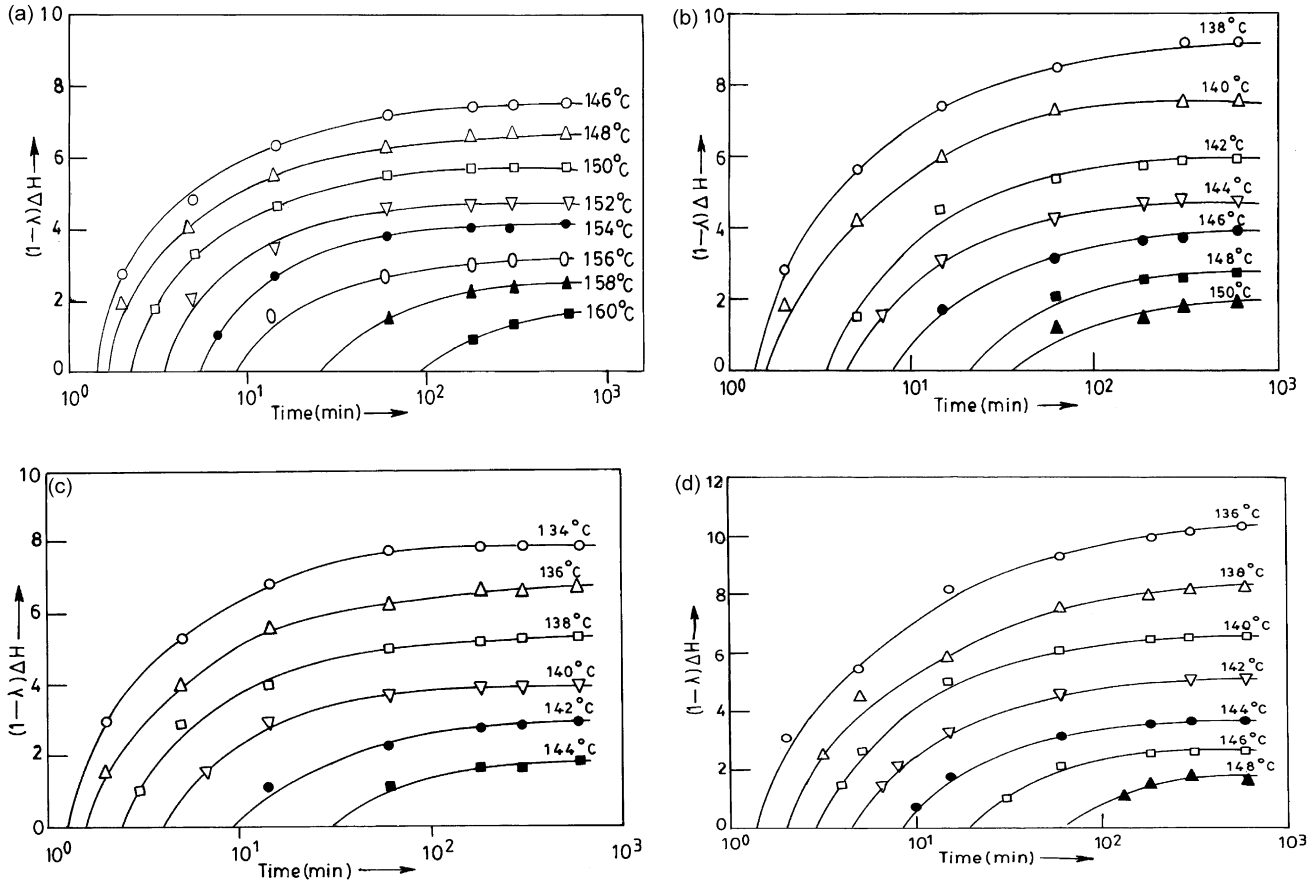

Fig. 4. Crystallization isotherms at indicated temperatures of P3OT(R)/P3HT(2) systems: (a) $W_{P3OT(R)}=0.0$ (b) $W_{P3OT(R)}=0.25$, (c) $W_{P3OT(R)}=0.5$ and (d) $W_{P3OT(R)}=0.75$.

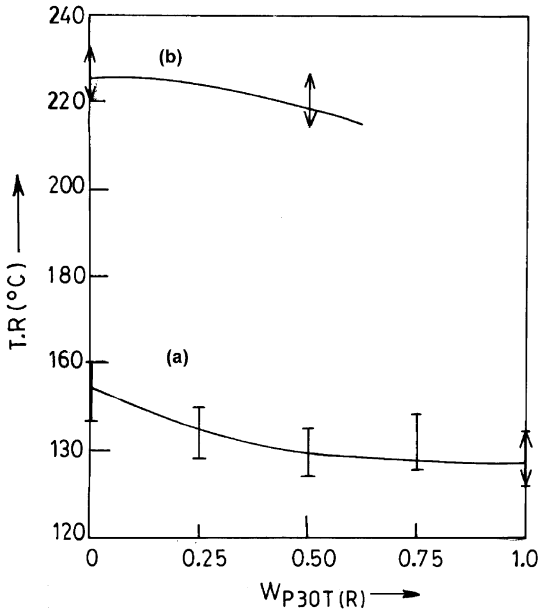

Fig. 5. Isothermal temperature range (TR) for the same time scale of crystallization vs weight fraction ofP3OT(R): (a) P3HT-2/P3OT(R) and (b) P3HT(R)/P3OT(R) systems.

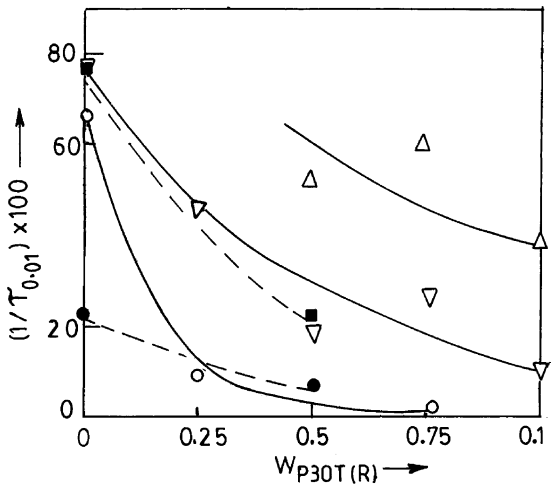

Fig. 6. $1/\tau_{0.01}$ ($\tau_{0.01}$ = time to obtain 1% crystallinity, computed from Figs. 2 and 3) vs weight fraction of P3OT(R) at same isothermal crystallization temperatures. Open symbol P3HT(R)/P3HT-2 and closed symbol P3HT-(R)/P3OT(R) systems (○, 146 °C; ▽, 140 °C; △, 136 °C); (●, 226 °C; ■, 220 °C).

Table 2
Values of Avrami exponents (n) ± 0.05 for P3OT(R)/P3HT-2 and P3HT(R)/P3OT(R) systems at different T_c values

P3OT(R)/P3HT-2										P3HT(R)/P3OT(R)			
$W_X=0.0$		$W_X=0.25$		$W_X=0.50$		$W_X=0.75$		$W_X=1.0$		$W_X=0.00$		$W_X=0.50$	
T_c (°C)	n	T_c (°C)	n	T_c (°C)	n	T_c (°C)	n	T_c (°C)	n	T_c (°C)	n	T_c (°C)	n
146	0.59	138	0.73	134	0.62	136	0.60	132	0.63	220	0.56	214	0.55
148	0.81	140	0.94	136	1.04	138	0.37	134	0.98	212	0.70	216	1.00
150	0.30	142	1.06	138	0.31	140	0.56	136	1.45	224	0.46	218	0.33
152	0.51	144	0.27	140	1.16	142	0.30	138	0.81	226	0.50	220	0.51
154	0.33	148	0.58	142	0.56	144	0.62	140	0.87	228	0.41	222	0.23
156	0.88							142	0.65	230	0.43		

3.3. Temperature coefficient analysis

The temperature coefficient analysis of the crystallization rate may be done from the Lauritzen–Hoffman growth rate equation [17]:

$$G = G_0 \exp\left[\frac{-U^*}{R(T-T_\infty)}\right]\exp\left[\frac{-K_g(i)}{T(\Delta T)}\right] \tag{3}$$

where G is the growth rate of the crystal, G_0 is the pre exponential factor, U^* is the activation energy of transport, $T_\infty = T_g - 30$, T_g is the glass transition temperature, T is the crystallization temperature, $\Delta T = T_m^0 - T$ where T_m^0 is the equilibrium melting point of the crystal and $K_g(\mathrm{I}) = 2K_g(\mathrm{II}) = K_g(\mathrm{III})$ with $K_g(\mathrm{I}) = 4b\sigma\sigma_e T_m^0/k\Delta H_f$, σ and σ_e are lateral and end surface energies, respectively, b is the thickness of the stem, k is the Boltzmann constant and ΔH_f is the enthalpy of fusion per unit volume. Here we consider $1/\tau_{0.01}$ to be G, where $\tau_{0.01}$ is the time required to obtain 1% crystallinity and is calculated from the crystallization isotherms.

In Fig. 7(a) and (b) $\ln 1/\tau_{0.01}$ values are plotted with $T_m^0/T(\Delta T)$ for the systems P3HT(R)/P3OT(R) and P3HT-2/P3OT(R), respectively. In both the figures the data of each blend cannot be presented by single line. Two different lines represent the data well and the ratio of the slopes of the two lines is approximately 2 for each case. The nature of the plots indicates regime-I to regime-II transition. The regime transition temperature and the undercooling calculated from the T_m^0 values of each blend are presented in Table 3. The regime transition temperature of both the systems gradually decreases with increasing the higher side chain length component. The undercooling at the regime transition temperature also decreases with increasing the concentration of larger side chain length.

The $\sigma\sigma_e$ values, calculated from the slopes of the straight lines, are presented in Table 4. It is clear from the table that $\sigma\sigma_e$ value gradually decreases with increasing the longer side chain length component. Here the σ_e values of pure components were calculated by dividing with the value of σ (12.4 erg/cm^2 for P3HT and 10.1 erg/cm^2 for P3OT) [18]. The σ_e values of the blends were taken as the arithmetic average of the component values and from these values the σ values of the blends are calculated and are also presented in Table 4. There is a gradual decrease of σ values with increasing concentration of larger alkyl group component for the P3HT(R)/P3HT-2 system. However, in the P3HT(R)/P3OT(R) system the 50:50 blend shows a sharp decrease in the σ value at both the regimes.

The lateral surface energy (σ) may be interpreted in two different ways [14]: (i) from the chain configuration viewpoint it relates to the chain characteristic ratio (C_α) at the melt by the relation:

$$\sigma = \Delta H_u^0\left(\frac{a}{2}\right)\left(\frac{l_b}{l_u}\right)\left(\frac{1}{C_\alpha}\right) \tag{4}$$

where l_b is the bond length of the monomer unit and l_u is the projected bond length of the monomeric unit along the chain direction (ii) from thermodynamic point of view it relates to the loss of entropy for the transformation of coil (I) to the activated state (II) prior to crystallographic attachment [13,14].

$$\Delta S_{\mathrm{I-II}} = \frac{2b\sigma l_u n^*}{T_m^0} \tag{5}$$

where n^* is the number of carbon atoms at the initial fold length.

3.4. Chain configuration of the melt

The C_α values of each system are calculated from the σ values for both the regimes from the Eq. (3) taking $a = 16.63$ Å, [25] $\Delta H_u^0 = 10.96 \times 10^8$ erg/cm^3, $l_b/l_u = 1.26$ (calculated from energy minimized MMX model [26]) and its plot with blend composition is shown in Fig. 8. For both the systems the C_α values shows a positive deviation from linearity calculated from both the regimes. The C_α value of pure melt is equal to $\bar{r}_0^2/nl_b^2$ where $\bar{r}_0^2$ is the mean square unperturbed end to end distance and n is the number of the monomeric unit in the chain [27]. In the melt of the cocrystals due to the favorable interaction of the components the P3HT chains may be extended by a factor α:

$$\alpha = \left(\frac{C_\alpha^{\mathrm{cocrystal}}}{C_\alpha^{\mathrm{pure}}}\right)^{1/2} \tag{6}$$

where $C_\alpha^{\mathrm{cocrystal}}$ is the chain characteristic ratio of the

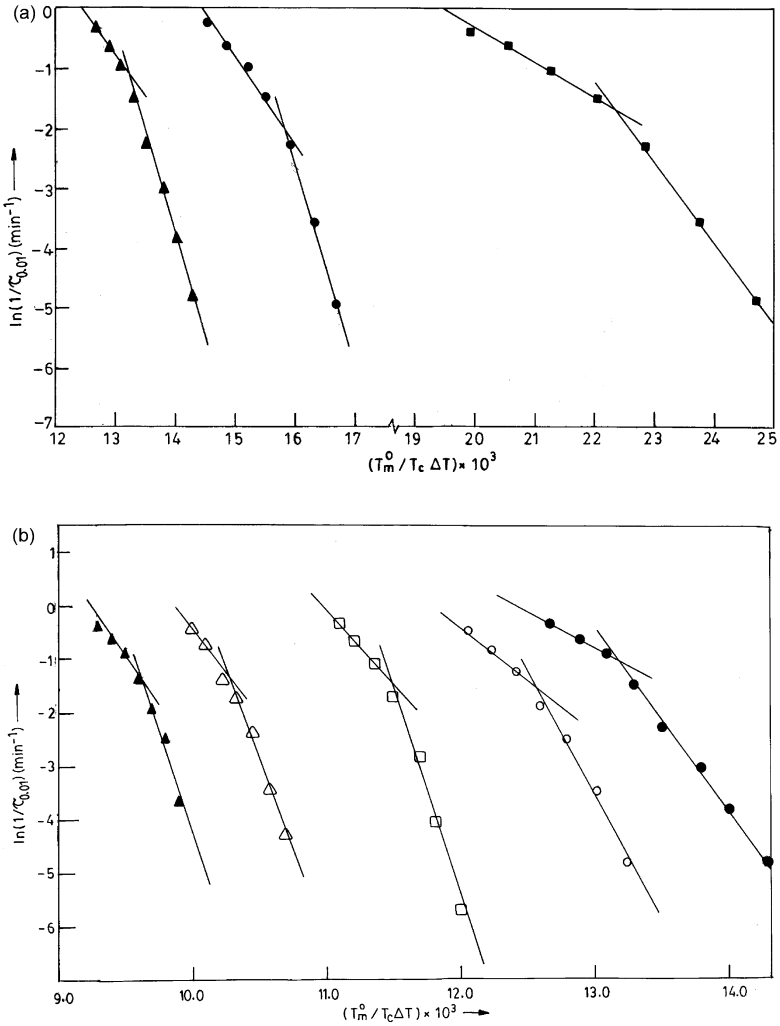

Fig. 7. (a) $\ln(1/\tau_{0.01})$ vs $T_m^0/T\Delta T$ plots of P3HT(R)/P3OT(R) cocrystals at different weight fraction of P3OT(R). ●, 0.0; ■, 0.50; ▲, 1.0. (b) $\ln(1/\tau_{0.01})$ vs $T_m^0/T\Delta T$ plots of P3OT(R)/P3HT-2 cocrystals at different weight fraction of P3OT(R). ▲, 0.00; △, −0.25; □, −0.50; ○, −0.75; ●, −1.0.

cocrystal and C_α^{pure} is the C_α value for the blend composition obtained from the line joining that of the components. The α values calculated from Eq. (6) are presented in Table 5. It is clear from the table that there is chain extension in the blends of both P3OT(R)/P3HT-2 and P3HT(R)/P3OT(R) systems. This is in accordance with the observation from the phase diagram [28], which denotes a small interaction in the P3HT-2/P3OT(R) system and this small interaction is the cause of small chain extension of the system. However, in the P3HT(R)/P3OT(R) blend the chain extension factor is comparatively larger. Such chain extension at the melt of crystalline–amorphous [29,30] and crystalline–crystalline polymer blends [12,13,31,32] were reported previously and the chain extension in polymer blends was also predicted from Monte Carlo (MC) simulation studies by Cifra et al. [33,34].

Table 3
Equilibrium melting point (T_m^0), regime-I to regime-II transition temperature (T_c^*) and their undercooling of P3OT(R)/P3HT-2 and P3HT(R)/P3OT(R) cocrystals

Sample composition (W_X)[a]	P3OT(R)/P3HT-2			P3HT(R)/P3OT(R)		
	T_m^0 (°C)	T_c^* (°C)	ΔT (°C)	T_m^0 (°C)	T_c^* (°C)	ΔT (°C)
0.00	290	152	138	300	227.9	72.1
0.25	270	140.7	129.3	–	–	–
0.50	250	136.5	113.5	270	220.6	49.4
0.75	240	140.4	99.6	–	–	–
1.00	230	138.8	91.2	230	138.8	91.2

[a] W_X = weight fraction of P3OT(R).

Table 4
$\sigma\sigma_e$ (erg^2 cm^{-4}); σ_e (erg cm^{-2}) and σ (erg cm^{-2}) values of P3OT(R)/P3HT-2 and P3HT(R)/P3OT(R) cocrystals calculated from slopes of Fig. 6(a) and (b), respectively

Sample composition $(W_X)^a$	P3OT(R)/P3HT-2						P3HT(R)/P3OT(R)					
	Regime-I			Regime-II			Regime-I			Regime-II		
	$\sigma\sigma_e$ (erg^2 cm^{-4})	σ_e (erg cm^{-2})	σ (erg cm^{-2})	$\sigma\sigma_e$ (erg^2 cm^{-4})	σ_e (erg cm^{-2})	σ (erg cm^{-2})	$\sigma\sigma_e$ (erg^2 cm^{-4})	σ_e (erg cm^{-2})	σ (erg cm^{-2})	$\sigma\sigma_e$ (erg^2 cm^{-4})	σ_e (erg cm^{-2})	σ (erg cm^{-2})
0.0	3573	287.4	12.4	3578	287.8	12.4	1525	122.6	12.4	1525	122.6	12.4
0.25	2468	245.5	10.0	2920	243.9	11.9	–	–	–	–	–	–
0.50	2410	203.6	11.5	2266	200.0	11.3	549	126.9	4.3	508	117.5	4.32
0.75	1773	170.2	10.4	1667	156.2	10.7	–	–	–	–	–	–
1.00	1213	119.7	10.1	1005	99.2	10.1	1213	131.1	10.1	1005	112.3	12.4

[a] W_X = weight fraction of P3OT(R).

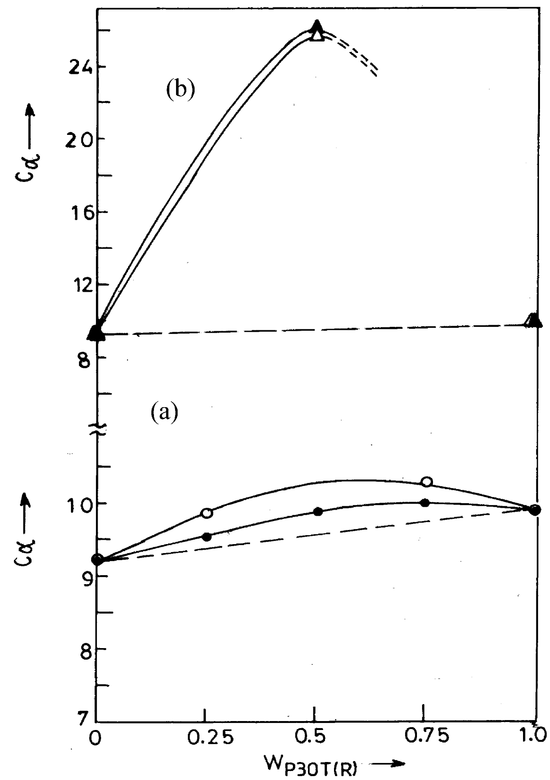

Fig. 8. Plot of chain characteristic ratio (C_α) against weight fraction of P3OT(R) for (a) P3OT(R)/P3HT-2 and (b) P3OT(R)/P3HT(R) systems (open symbol from regime-I data and closed symbol from regime-II data) [in Fig. 8(b) the curve is not completely drawn due to phase separation at $W_{P3OTR}=0.86$ [7,28]].

3.5. Entropy of cocrystallization

The entropy of activation (ΔS_{I-II}) has been calculated from Eq. (5) taking $b=7.75\times10^{-8}$ and 7.64×10^{-8} cm for P3HT and P3OT, respectively, $n^*=1.7\times10^{22}$ and 1.62×10^{22} carbon and sulfur atoms for P3HT and P3OT, respectively, (calculated for P3HT, $a=16.6\times10^{-8}$ cm, $b=7.75\times10^{-8}$ cm and monomeric bond length $=5.03\times10^{-8}$; for P3OT, $a=20.9\times10^{-8}$ cm, $b=7.64\times10^{-8}$ and monomeric bond length $=5.03\times10^{-8}$). For the blends the arithmetic average values were taken for each composition. The entropy of activation values (Table 5) are negative indicating that the disorderliness of the chain has decreased during the formation of activated state (localized state) [12, 13]. The entropy of activation is plotted in Fig. 9(a) and (b) for P3HT-2/P3OT(R) and P3HT(R)/P3OT(R) systems, respectively. In the former systems the plot shows a negative deviation from linearity while in the later system there is a positive deviation from linearity joining the component values. This indicates that in the P3HT-2/P3OT(R) blends the activated state formation causes larger entropy loss than that of pure components. But the P3HT(R)/P3OT(R) systems present the usual observation observed in other cocrystal systems. The entropy of cocrystallization (ΔS_c) is calculated from the equation

Table 5
Chain extension factor (α), entropy of activation (ΔS_{I-II}) and entropy of cocrystallization ($\Delta S_{cocrystal}$) of P3OT(R)/P3HT-2 and P3HT(R)/P3OT(R) cocrystals

Cocrystal composition (W_x)*	P3OT(R)/P3HT-2						P3HT(R)/P3OT(R)					
	Regime-I			Regime-II			Regime-I			Regime-II		
	α	ΔS_{I-II} (e.u)	$\Delta S_{cocrystal}$ (e.u)	α	ΔS_{I-II} (e.u)	$\Delta S_{cocrystal}$ (e.u)	α	ΔS_{I-II} (e.u)	$\Delta S_{cocrystal}$ (e.u)	α	ΔS_{I-II} (e.u)	$\Delta S_{cocrystal}$ (e.u)
0.00	1.00	−8.12	0.00	1.00	−8.12	0.00	1.0	−8.0	0.00	1.00	−8.0	0.00
0.25	1.04	−8.2	−0.30	1.02	−8.52	0.60	–	–	–	–	–	–
0.50	1.01	−10.55	–	1.02	−8.6	−0.9	1.64	−3.13	4.65	1.65	−3.13	4.6
0.75	1.10	−8.32	−1.10	1.01	−8.3	−1.12	–	–	–	–	–	–
1.00	1.00	−7.34	0.00	1.00	−7.34	0.00	1.00	−7.34	0.00	1.00	−7.34	0.00

* W_X = weight fraction of P3OT(R).

$$\Delta S_c = \Delta S_{I-II}^{cocrystal} - \Delta S_{I-II}^{pure} \quad (7)$$

where ΔS_{I-II}^{pure} is meant the entropy of activation of pure state and has been computed from the dotted line joining that of the components. ΔS_c exhibits a negative value for P3HT-2/P3OT(R) systems but the P3HT(R)/exhibits a positive value. Thus, it may be concluded from these results that cocrystallization of P3HT(R)/P3OT(R) system is an entropy driven process [12,13] whereas that of P3HT-2/P3OT(R) system is an entropy forbidden process. A possible reason that may be afforded in the P3HT-2/P3OT(R) system where both regioregularity and side chain length vary but in P3HT(R)/P3OT(R) system only the side chain length vary. It might be probable that in the former system the combined variation of regioregularity and side chain length produce a more ordered structure than that in the cocrystals of P3HT(R)/P3OT(R) where some disorderliness appears during cocrystallization. Though in the P3HT-2/P3OT(R) system cocrystallization is entropy forbidden but the small interaction (as concluded from phase diagram [28]) between the components overcome the small entropy effect and cocrystallization is observed for the whole composition range.

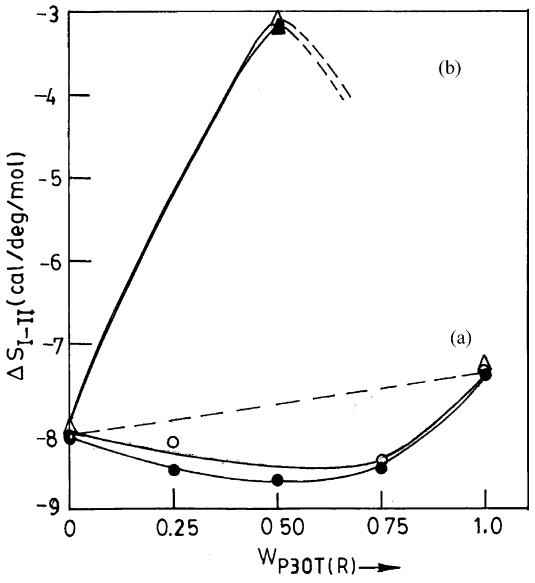

Fig. 9. Plot of entropy of activation (ΔS_{I-II}) vs weight fraction of lower melting component (a) P3OT(R)/P3HT-2 and (b) P3HT(R)/P3OT(R) systems (open symbol from regime-I data and closed symbol from regime-II data) [in Fig. 9(b) the curve is not completely drawn due to phase separation at $W_{P3OTR} = 0.86$ [7,28]].

4. Conclusion

This study clearly indicates that overall crystallization rate of the cocrystals decreases with increasing side chain length at same isothermal crystallization temperature. The crystallization mechanism in the pure components and also in the cocrystals is the same. The low value of Avrami exponent (0.23–1.16) arises from the soft impingement with the rigid amorphous portion and also from the non-negligible value of nuclei volume fraction during the crystallization process. In both the blends and its components there is regime-I to regime-II transition. The $\sigma\sigma_e$ values decrease with increasing the concentration of longer alkyl chain length of P3AT. Analysis of the $\sigma\sigma_e$ values indicates that there is chain extension in all the blends, however, the entropy of cocrystallization has different sign to the two systems. The P3HT(R)/P3OT(R) system is entropy driven process whereas P3HT-2/P3OT(R) is entropy forbidden process. Possible explanation for cocrystallization in the later system has been attributed from the small interaction between the components as evidenced from the phase diagram.

Acknowledgements

We gratefully acknowledge Council of Scientific and Industrial Research, New Delhi (Grant No. 1655/00/EMR-II) for financial support.

References

[1] McCullough RD, Ewbank PC. In: Skotheim TA, Elsenbaumer RL, Renolds JR, editors. Handbook of conducting polymers. New York: Marcel Dekker; 1998. p. 225.
[2] Roncali J. Chem Rev 1992;92:711.
[3] Yoshino K, Park DH, Park BK, Fujii M, Sugimoto R-I. Jpn J Appl Phys 1988;27:L1410.
[4] McCullough RD, Lowe RD, Jayaraman M, Anderson DJ. Org Chem 1993;58:904.
[5] Chen T-A, Wu X, Rieke RD. J Am Chem Soc 1995;117:233.
[6] Faid K, Frechette M, Ranger M, Mazerolle L, Levesque I, Leclerc M, et al. Chem Mater 1995;7:1930.
[7] Pal S, Nandi AK. Macromolecules 2003;36:8426.
[8] Ree M. PhD Thesis. Amherst, USA: University of Massachusetts; 1987.
[9] Iragorri JJ, Rego JM, Katime I, Conde Brana MT, Gedde UW. Polymer 1992;33:461.
[10] Tashiro K, Izuchi M, Kaneuchi F, Jin C, Kobayashi M, Stein RS. Macromolecules 1994;27:1240.
[11] Tashiro K, Imanishi K, Izumi Y, Kobayashi M, Kobayashi K, Satoh M, et al. Macromolecules 1995;28:8477.
[12] Datta J, Nandi AK. Polymer 1998;39:1921.
[13] Datta J, Nandi AK. Macromol Chem Phys 1998;199:2583.
[14] Hoffman JD, Miller RL, Marand H, Rotiman DR. Macromolecules 1992;25:2221.
[15] Ihn JK, Moulton J, Smith P. J Polym Sci, Part B: Polym Phys 1993;31: 735.
[16] Mena-Osteriz E, Meyer A, Langeveld-voss BMW, Janssen RAJ, Meizer EW, Bauerie P. Angew Chem Int Ed 2000;39:2680.
[17] Hoffman JD, Davis GT, Lauritzen JL. In: Hannay NB, editor. Treatise on solid state chemistry, vol. 3. New York: Plenum Press; 1976. p. 497.
[18] Malik S, Nandi AK. J Polym Sci, Polym Phys Ed 2002;B40:2073.
[19] Avrami M. J Chem Phys 1939;7:1103. Avrami M. J Chem Phys 1940; 8:212.
[20] Von Golar F, Sachs G. Z Phys 1932;77:281.
[21] Mandelkern L. Crystallization of polymers. New York: McGraw-Hill; 1964.
[22] Nascimento OR, Correa AA, Bulhoes LOS, Perira EC, Puwlicke A, Walmsley L. J Chem Phys 1998;109:8729.
[23] Cheng SZD, Wunderlich B. Macromolecules 1988;21:3327.
[24] Cheng SZD. Macromolecules 1988;21:2475.
[25] Tashiro K, Ono K, Minagawa Y, Kobayashi M, Kawai T, Yoshino K. J Polym Sci, Polym Phys 1991;B29:1223.
[26] Gajewski KE, Gillberr MH. In: Liotta D, editor. Advances in molecular modelling, vol. 2. Greenerick, CT: Jai Press; 1990.
[27] Flory PJ. Statistical mechanics of chain molecules. New York: Interscience Publishers; 1969.
[28] Pal S, Nandi AK. J Phys Chem B 2005;109:2493.
[29] Huang J, Prasad A, Marand H, Roitman DB. Polymer 1994;35:1896.
[30] Maiti P, Nandi AK. Polymer 1998;39:413.
[31] Rahman MH, Nandi AK. Polymer 2002;43:6863.
[32] Rahman MH, Nandi AK. J Polym Sci, Polym Phys 2004;B42:2215.
[33] Cifra P, Karasz FE, Macknight WJ. J Polym Sci, Polym Phys 1988; B26:2379.
[34] Cifra P, Karasz FE, Macknight WJ. Macromolecules 1992;25:192.